

Experimental study of charge injection from gold/aluminium into regioregular poly (3-hexylthiophene)

دراسة تجريبية لحقن الشحنات من الذهب / الألمنيوم rrP3HT - كداله لطول قناة القطبين

Bestoon T. Mustafa, Dr. Hewa Y. Abdullah, Saman Q. Mawlood
Department of Physics/ college of education, University of Salahaddin,
Bagdad Road, Kurdistan Region

Abstract:

The nature of charge injection has been investigated across the gold (Au) / aluminium (Al) - regioregular poly(3-hexylthiophene), rrP3HT, interface as a function of channel length of the two electrodes. The sheet resistance (R_{\square}) of rrP3HT in contact with Au/Al electrodes and contact resistance (bottom contact and top contact) are also measured. Sheet resistance was found to be $8 \times 10^8 \Omega/\square$. The total resistance (R_t) increases from 12.5 to 33 M Ω as the channel length (L) increases between 20 and 80 μm at room temperature. The I-V characteristics of a Au (bottom)/P3HT/Au (top) sandwich cell and Al/P3HT/Al contacts are analyzed by using the Keithley source-measure unit for all samples separately and the hole barrier height at the top and bottom contacts has been estimated. I-V curve shows ohmic contact and nonohmic properties (nonlinear) of the Au/P3HT/Au and Al/P3HT/Al interfaces respectively.

Key word: energy level alignment, interface, total and sheet resistance, ohmic and nonohmic contact.

الخلاصة:

تم دراسة طبيعة حقن الشحنة عبر السطح البيني الذهب / الألمنيوم - rrP3HT كداله لطول قناة القطبين. كذلك تم قياس المقاومة السطحية (R_{\square}) لوصلة المفرق (التماس) Au/Al - rrP3HT ومقاومة التماس (السفلي و العلوي). وكانت قيم المقاومة السطحية ($8 \times 10^8 \Omega/\square$). المقاومة الإجمالية (R_t) تزداد (12.5 - 33 M Ω) بزيادة طول القناة (L) ما بين 20 و 80 ميكرون في درجة حرارة الغرفة. وتم تحليل خصائص (تيار- الفولتية) لوصلة التماس (السفلي و العلوي) Au/P3HT/Au ووصلة التماس Al/P3HT/Al باستخدام وحدة قياس Keithley لجميع العينات بشكل منفصل وكذلك تم تقييم ارتفاع حاجز الجهد للفجوات للتماس (السفلي و العلوي). وتبين من منحني (تيار- الفولتية) ان طبيعة التماس لهذه النماذج تمتلك خصائص أومية (Au/P3HT/Au) وخصائص وغير اومية (Al/P3HT/Al) (غير خطية) على التوالي.

Introduction:

Organic semiconductor materials have attracted considerable attention recently in solution-processable electronic devices such as field effect transistors (FETs) and organic light emitting diodes (OLEDs). This is due to their unique electrical and optical properties and low fabrication cost comparable to inorganic semiconductor based devices [1, 2, 3, 4]. Nowadays, however, inorganic semiconductors are not being widely used due to their high cost [5]. Organic semiconductor devices, on the other hand, suffer from low stability, short device lifetime and poor performance [6]. Consequently, studies have been conducted to bring high efficient and low cost organic semiconductor devices into operation. The interfaces of metal/organ and organ/metal have attracted much interest to the rapid development of the organic electronic devices and wiring of future molecular devices [7, 8, 9]. Regarding to the metal/organ interfaces, device performances, in addition, depends on the fabricating processes well as the environmental factors (such as depositing and annealing temperature), have an impact on the carrier motilities throughout the device [2, 3].

The subject of interfacial electronic structure covers two aspects: (i) the energy level alignment at the metal/organic interface (or organ/metal interface) forms a dipole layer and, (ii) the band bending. To describe the electronic structure at the metal/organ interface, a Mott–Schottky’s model can be employed and accordingly: (i) a common vacuum level produces between the metal/organic interface and (ii) Fermi level aligns between the metal and the organic semiconductor when they come into contact [10]. The dipole layer forms as a consequence of the charge transfer (CT) across the interface, electron cloud redistribution and interfacial chemical reaction. Across the dipole layer, the interfacial potential is led to an abrupt shift as a consequence of the interfacial Dipole formation. Consequently, the virtual vacuum level (VL) shifts at the metal and organic interface and this leads to shift the VL in the organic layer. The surface science field will explain the shift of VLs (VL at the solid surface), and can be described by changes in the work functions and/or surface potential of the metal. This occurs whereas there area deposition and an adsorption of organic semiconductor molecules above a metal surface [10, 11, 12].

Previous studies show the current limitation due to the injection limited carriers across the interface (called injection limited current) if the metal/organic interface barrier is larger than 0.3 eV at zero electric field. Whereas, for a potential barrier with less than a 0.3 eV, the injection barrier will be small and the carriers are injected efficiently into the device. Thus, the charge transfer will be limited through the bulk material of the device, termed the bulk transport limited [13, 14, 15].

Recently, the p-type conjugated organic polymers have a promising role in electronic applications such as organic light emitting diode, thin film transistors and solar cells [8, 16, 17]. The P3HT is one of the most potential conducting polymers which behaves as a p-type semiconductor. It mostly comes into contact with gold (Au) or aluminium (Al) owing to their high work function [18, 19, 20]. Regioregular poly (3-hexylthiophene) is mostly utilized organic semiconductor in organ electronic devices due to its desirable electronic properties and high field-effect mobility [21, 22]. An easy approach to deposit the organic materials is spin casting [3]. It forms a thin film with a good morphology surface, and its thickness can be easily controlled by changing the spin speed. In devices such as organic photo voltages (OPVs), P3HT is blended with another polymer solution and spin coated as the active region of the device [1, 2, 3]. While, in devices such as thin film transistors the polymer is deposited as itself (to deposit a thin film) in order to extracting p-type carries as the gate voltage is applied [23]. Here, a single film of rrP3HT will be spin coated above Al or Au electrodes.

However, Very recently, a contact resistance was observed in field-effect transistor (TFTs) geometries with Au metal electrodes [19]. Yet, there are still lacking of the detailed studies of the Au/P3HT contact properties. In this paper we show: (i) the electrical property of metal (Au and Al)/rrP3HT contacts by showing the current–voltage characteristics and, (ii) The sheet resistance of the rrP3HT thin films at room temperature. Our analysis reveals the ohmic contact and nonohmic contact of Au and Al/rrP3HT contact electrodes respectively.

The organization of this paper is as follows. First, the contact properties of metal/rrP3HT have been discussed. Experimental section will be detailed next and then the experimental result of sheet and total resistance of P3HT thin films versus their channel length will be discussed. Finally, we summarized our conclusions.

Material and Method:

To prepare the rrP3HT thin films, the polymer (P3HT) (%96.6 pure) was purchased from Sigma Aldrich and was dissolved in chloroform at a concentration of 10 mg/mL. rrPEHT films were then deposited above Al and Au coated glass substrates. The substrates were cleaned (prier the film deposition) in de-ionized water and Hellmanex and sonicating for 20 min at 70 °C. After sonication, the substrates were washed down with the de-ionized water. They were then put in iso-propanol and sonicated for 20 min at 70 °C. Finally, the washed substrates were dried with nitrogen gas.

Solution preparation of P3HT was made in a dim light and heated at 45 °C for 15 minutes (with help of magnetic stirrer). In order to reduce impurities, the solvent was then filtered prior deposition. Thin films of P3HT were deposited via spin coating onto cleaned Al and Au substrates and were annealed at 40 °C for one hour in air. Self-assembling thin films of regioregular poly (3-hexylthiophene) were formed onto the Al and Au substrates, observed with optical microscopy. The thickness of Al and Au are 100 nm and 50.5 nm respectively. Au and Al electrodes were used with different channel length (20, 40, 60 and 80 μm). After deposition of the thin film, samples were encapsulated using an inert UV curable epoxy and a glass cover slide. The I-V characteristics were measured using a Keithley 2400 source meter under ambient conditions. An NREL calibrated silicon diode was used to calibrate the power output at 100 mW/cm². The bias voltage has been set from 30 to -30 V.

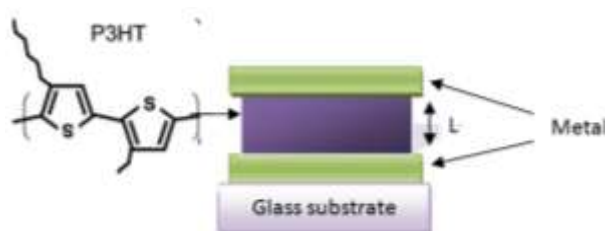


FIG. 1. Sample geometries and the chemical composition of the rrP3HT, L represents the channel length (the distance between the two metal electrodes). Both metal electrodes can be either Al or Au.

Result and Discussion:

Figure 2 shows the current-voltage characteristics of the samples with different channel length with a use of rrP3HT film as the hole extraction layer. The electrical properties of Au in contact to rrP3HT films are shown in Figure 2(a), films have been deposited above the Au substrates with 20, 40, 60 and 80 μm channel length. The results are listed in table 1, thin films which possess the same structure properties (thickness and depositing condition) show a dramatic increase of total resistance of the samples as the channel length is increased. The total resistance was 12.5 MΩ recorded as the practical channel length 22.75 μm (20 μm theoretical value) is used. This resistance has increased into 25 then 33 MΩ where a 59.5 (experimental value versus 60 μm theoretically) and 76.5 μm (experimental value versus 80 μm theoretically) are employed respectively. The sheet resistance also increased continuously as the channel length increased (table 1). This is consistent with that which carriers should cross a wider distance to from the bulk material (film) to reach into the other electrode and a higher resistivity is loaded against the injected carriers from the below Au metal (see below). The total sheet resistance were also calculated is $8 \times 10^8 \Omega/\square$. The raise of the total resistance returns to the fact that the rrP3HT film possesses a higher bulk limitation property of the film as L increases.

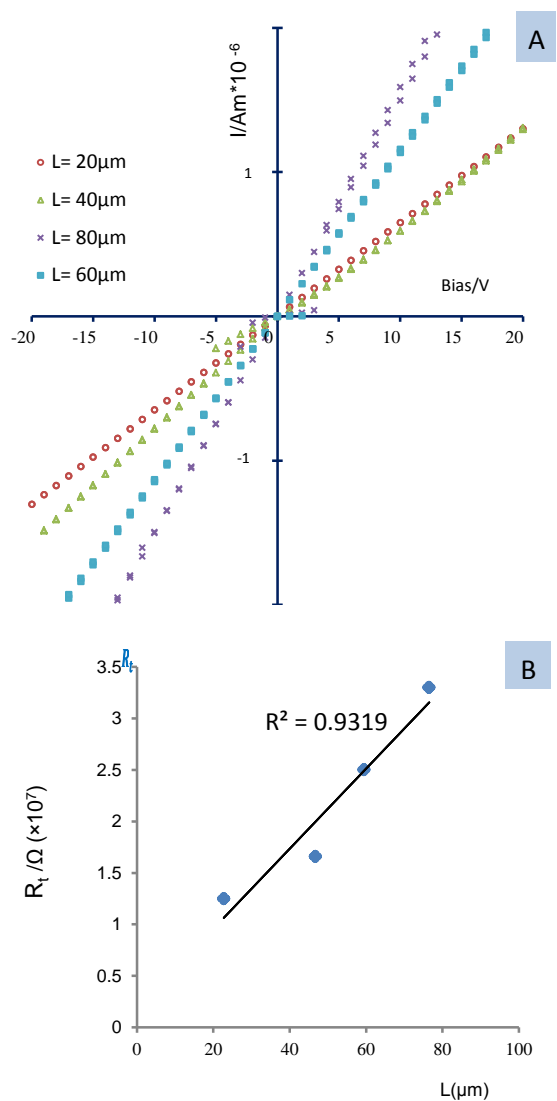


FIG. 2. (a) The current - voltage characteristics of rrP3HT samples, is shown for rrP3HT films in contact with Au electrodes as a function of channel length, circles 20 μm , unfilled triangles 40 μm , filled squares 60 μm and crosses 80 μm) and (b) is the relation between the channel length and the total resistance.

Table 1. The average experimental values of total resistance and the sheet resistance are shown with the standard error. 1/Slope represents the total resistance.

$L (\mu m)$	$(A/V) \times 10^{-8}$ Amp/V	(R_t) $M\Omega$	$R_{\square} [\Omega/ \square] \times 10^8$
22.75 ± 0.13	8 ± 0.009	12.5 ± 0.4	11
46.75 ± 0.16	6 ± 0.009	16.6 ± 0.4	7
59.50 ± 0.004	4 ± 0.009	25.0 ± 0.4	8
76.50 ± 0.04	3 ± 0.009	33.0 ± 0.4	9

Figure 2(b) shows samples total electrical resistance R_t versus channel length using films that were deposited on Au substrates. It shows the dramatic increase of the total resistance as the channel length increases. From the figure 2 (b), the total resistance, contact resistances and the sheet resistance were measured by applying equation 1 (see below). The sheet resistance is much bigger

than the contact resistance. This reveals the bulk limitation property of the sample rather than injection limitation.

The injection of charge carriers from the gold contacts to the organic semiconductor polymer has not formed a high electrical barrier (figure 1a). This is expected when Au/P3HT come to interface, due to the energetically ideal compatibility of Au work-function (ϕ) (5.1 eV shown in literature [24]) to the highest occupied molecular orbital (HOMO) state in the P3HT conjugated polymer. In addition, the linearity reveals the bulk limitation (small injection barrier at the interface) of injecting a current where Ohm law is valid. This is a significant indication to show a free trap for transport holes. Moreover, the symmetric linearity observation with no hysteresis indicates a film free of oxygen dopants. There is, however, a strong connection between an increase in the concentration of O₂ dopants and expose the deposited film to the atmosphere throughout the spin coating process in some types of p-type semiconductor polymers. Hence the production of nonlinearity at rrP3HT/Au interface has been reported in ref [8].

For the p-type semiconductor, used in electronic devices, the work function of the metal should be equal or larger than the band gap of the organic. The work function of polycrystalline Au is about 5.1eV and this is below the HOMO level of rrP3HT (recorded 4.8eV or 4.3 eV (5.1 eV was also found quite recently [25]), in literature [19, 26]) and the Fermi level of Au metal located well within the valence-band of rrP3HT. As a result, the mismatch of rrP3HT organic layer and Au metal Fermi energy becomes low and that causes a lower-resistance rectifying contact. This is the criterion for ohmic contacts in which a sufficient charge carriers can be ejected from the contacts (holes in case of rrP3HT) to enter the bulk material and causes space-charge limited regime [8, 9]. When a voltage is applied, carriers eject between electrodes and pass from the organic layer, the Schottky barrier is low between Au and rrP3HT.

$$R_t = R_1 + R_2 + L \frac{R_{\square}}{W} \dots\dots\dots (1)$$

From equation 1, R_t is the total resistance, R_1 and R_2 are contact resistances at the electrodes/semiconductor interface, R_{\square} is the sheet resistance and it is measured by Ω/\square or Ω/square , W (2 mm) is electrode width and L is channel length. Equation 1 can be represented by a straight-line equation $y = mx + b$. Where m represents the value of the slope (found to be $4 \times 10^{11} \Omega m^{-1}$) of each single I-V curve and b is the y intercept that represents the value of $R_1 + R_2$ in figure 2 (b), found to be $2 \times 10^6 \Omega$. $1/\text{slope}$ in figure 2 (a) corresponds to the total contact resistance R_t for electrodes which increased by increasing the distance between electrodes (see above). Slope multiplied to W is the sheet resistance (found to be $R_{\square} = 8 \times 10^8 \Omega/\square$), of the rrP3HT organic thin film (shown in figure 2 (b)).

However, Al/rrP3HT/Al contacts show nonohmic contact for all samples with different channel length (figure 3). The ohms law cannot be applied, non-linearity of I-V curve. The nonlinearity reveals existence of a high Schottky energy barrier at Al/rrP3HT interface. This is due to the mismatch characteristics of the metal Fermi level versus the HOMO of the rrP3HT, (4.28) [27] and (4.8)eV [19] respectively as reported in literature) which limits the current injection into the organic layer. The carrier-injection barrier to jump holes at the Al electrode is about 0.9eV in contrast to only about 0.1eV in Au/rrP3HT interface as reported in literature [28]. This high-energy barrier gives difficulty to move holes between the two Al electrodes. Yet, to make an ohmic contact (reducing the potential barrier at The Al/P3HT contacts), a high doping rate is required, altering nonlinear behaviour can be allowed by applying a high voltage on the Al electrodes (seen in figure 3 at a high voltage doping rate). Unlikely, applying voltage has limitation. In diodes, a high doping rate makes the depletion layer narrower and allows flowing electrons easily and tunnelling through the barrier. In some organic transistors such as TFTs, the only technique of doping is possible with employing a voltage.

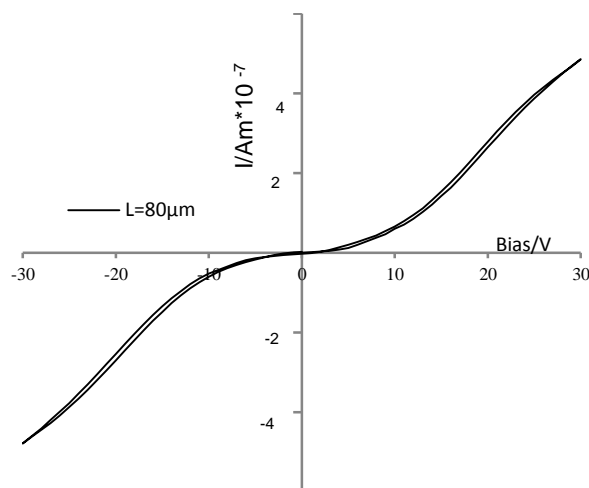


FIG. 3. Current /voltage characteristics of Al/rrP3HT/Al contacts at room temperature. The hysteresis shapes became narrower as the channel lengths increase from 20 to 80 μm , here; the channel length with only a 80 μm is platted. Applying a high voltage reduces the nonlinearity.

Generally, the nature of charge transport (P-and n-type) for either bulk limited or injection limited transport in devices can be determined by the range of the Schottky barrier. It is believed that the low work function of Al consequences a considerable Schottky energy barrier to inject the p type carriers in through the interface into rrP3HT polymer.

From studying the I-V characteristics of both Al/P3HT/Al and Au/P3HT/Au samples (fig. (3) and fig. (2)) allow us to distinguish between contact-limited from bulk-limited transport. We can demonstrate that a significant injection barrier forms at Al/rrP3HT contact a low doping level and it can be reduced as the dopant is increased. The contact resistance with Al electrodes is all change similarly at all channel length. The results also show the capability to control the doping level in organic semiconductors as a tool to investigate the electronic properties of devices. We also have observed significant hysteresis (fig. 3) in our curves while sweeping the voltage between negative to positive and back again. As expected, in both cases, a strong asymmetry is present. The asymmetry is such that injection of holes from the Al is less efficient than from Au, correspondence with expectations on the basis of the work-function of Al (smaller) compared to Au (5.1 eV).

Conclusion:

We have shown the contact electrical resistance of Au/rrP3HT and Al/rrP3HT contacts as a function of channel length. I-V curves of Au at contact to rrP3HT has shown an ohmic contact and low contact resistance (small potential barrier between the metal Au and the p-type polymer). The sheet resistance of rrP3HT ($8 \times 10^8 \Omega/\square$) led to a bulk charge limitation transport and it increased as the channel length has increased. However, the electrical properties for Al in contact to rrP3HT has also investigated in which a high injection barrier was observed (at a low doping level) for all channel length against the injection carrier from Al into the polymer. The hysteresis characteristic represents an injection limitation versus lower bulk limitation compare to Au electrodes. This makes Au to be more reliable to be used in depositing devices such as TFTs.

Acknowledgment:

The research was conducted at Sheffield University/UK. We would like to thank the teachers and Phd students who provided the polymer and use the laboratories. The research is a part of a self-coming idea during a high degree of study.

References:

1. Li, G., Shrotriya, V., Huang, J., Yao, Y., Moriarty, T., Emery, K., & Yang, Y. (2005). High-efficiency solution processable polymer photovoltaic cells by self-organization of polymer blends. *Nature materials*, 4(11), 864-868.
2. Nelson, J. (2011). Polymer: fullerene bulk heterojunction solar cells. *Materials today*, 14(10), 462-470.
3. Brabec, C. J., & Durrant, J. R. (2008). Solution-processed organic solar cells. *MRS bulletin*, 33(07), 670-675.
4. Steirer, K. X., Chesin, J. P., Widjonarko, N. E., Berry, J. J., Miedaner, A., Ginley, D. S., & Olson, D. C. (2010). Solution deposited NiO thin-films as hole transport layers in organic photovoltaics. *Organic Electronics*, 11(8), 1414-1418.
5. Li, Z., Zhao, X., Lu, X., Gao, Z., Mi, B., & Huang, W. (2012). Organic thin-film solar cells: Devices and materials. *Science China Chemistry*, 55(4), 553-578.
6. Brédas, J. L., Norton, J. E., Cornil, J., & Coropceanu, V. (2009). Molecular understanding of organic solar cells: the challenges. *Accounts of chemical research*, 42(11), 1691-1699.
7. Romaner, L., Heimel, G., Brédas, J.-L., Gerlach, A., Schreiber, F., Johnson, R. L., . . . Zojer, E. (2007). Impact of bidirectional charge transfer and molecular distortions on the electronic structure of a metal-organic interface. *Physical review letters*, 99(25), 256801.
8. Hamadani, B. H., Ding, H., Gao, Y., & Natelson, D. (2005). Doping-dependent charge injection and band alignment in organic field-effect transistors. *Physical Review B*, 72(23), 235302.
9. Scott, J. C., & Malliaras, G. G. (1999). Charge injection and recombination at the metal-organic interface. *Chemical physics letters*, 299(2), 115-119.
10. Ishii, H., Sugiyama, K., Ito, E., & Seki, K. (1999). Energy level alignment and interfacial electronic structures at organic/metal and organic/organic interfaces. *Advanced Materials*, 11(8), 605-625.
11. Koch, N. (2007). Organic electronic devices and their functional interfaces. *ChemPhysChem*, 8(10), 1438-1455.
12. Koch, N., Kahn, A., Ghijssen, J., Pireaux, J. J., Schwartz, J., Johnson, R. L., & Elschner, A. (2003). Conjugated organic molecules on metal versus polymer electrodes: Demonstration of a key energy level alignment mechanism. *Applied Physics Letters*, 82(1), 70-72.
13. Davids, P. S., Campbell, I. H., & Smith, D. L. (1997). Device model for single carrier organic diodes. *Journal of applied physics*, 82(12), 6319-6325.
14. Malliaras, G. G., & Scott, J. C. (1999). Numerical simulations of the electrical characteristics and the efficiencies of single-layer organic light emitting diodes. *Journal of applied physics*, 85(10), 7426-7432.
15. Mahapatro, A. K., & Ghosh, S. (2007). Charge carrier transport in metal phthalocyanine based disordered thin films. *Journal of applied physics*, 101(3), 034318.
16. Newman, C. R., Frisbie, C. D., da Silva Filho, D. A., Brédas, J. L., Ewbank, P. C., & Mann, K. R. (2004). Introduction to organic thin film transistors and design of n-channel organic semiconductors. *Chemistry of materials*, 16(23), 4436-4451.
17. Katz, H. E. (1997). Organic molecular solids as thin film transistor semiconductors. *J. Mater. Chem.*, 7(3), 369-376.

18. Hamadani, B. H., & Natelson, D. (2005). Nonlinear charge injection in organic field-effect transistors. *Journal of applied physics*, 97(6), 064508.
19. Rep, D. B. A., Morpurgo, A. F., & Klapwijk, T. M. (2003). Doping-dependent charge injection into regioregular poly (3-hexylthiophene). *Organic Electronics*, 4(4), 201-207.
20. Lei, C. H., Das, A., Elliott, M., Macdonald, J. E., & Turner, M. L. (2004). Au-poly (3-hexylthiophene) contact behaviour at high resolution. *Synthetic metals*, 145(2), 217-220.
21. Irwin, M. D., Buchholz, D. B., Hains, A. W., Chang, R. P., & Marks, T. J. (2008). p-Type semiconducting nickel oxide as an efficiency-enhancing anode interfacial layer in polymer bulk-heterojunction solar cells. *Proceedings of the National Academy of Sciences*, 105(8), 2783-2787.
22. Duraisamy, N., Muhammad, N. M., Hyun, M. T., & Choi, K. H. (2013). Structural and electrical properties of P3HT: PCBM/PEDOT: PSS thin films deposited through electrohydrodynamic atomization technique. *Materials Letters*, 92, 227-230.
23. Li, Z. L., Yang, S. C., Meng, H. F., Chen, Y. S., Yang, Y. Z., Liu, C. H., ... & Lee, R. H. (2004). Patterning-free integration of polymer light-emitting diode and polymer transistor. *Applied physics letters*, 84(18), 3558-3560.
24. Bürgi, L., Richards, T. J., Friend, R. H., & Sirringhaus, H. (2003). Close look at charge carrier injection in polymer field-effect transistors. *Journal of Applied Physics*, 94(9), 6129-6137.
25. Wang, Y., Tong, S. W., Xu, X. F., Özyilmaz, B., & Loh, K. P. (2011). Interface Engineering of Layer-by-Layer Stacked Graphene Anodes for High-Performance Organic Solar Cells. *Advanced Materials*, 23(13), 1514-1518.
26. Mikalo, R. P., & Schmeißer, D. (2002). Electric contacts on conductive polymers: sodium on poly (3-hexylthiophene-2, 5-diyl). *Synthetic metals*, 127(1), 273-277.
27. Hung, L. S., Tang, C. W., & Mason, M. G. (1997). Enhanced electron injection in organic electroluminescence devices using an Al/LiF electrode. *Applied Physics Letters*, 70(2), 152-154.
28. Liu, J., Yin, Z., Cao, X., Zhao, F., Lin, A., Xie, L., ... & Huang, W. (2010). Bulk heterojunction polymer memory devices with reduced graphene oxide as electrodes. *ACS nano*, 4(7), 3987-3992.